Supplementary Information

Microstructure-Dependent Particulate Filtration Performance of Multifunctional Metallic Nanowire Foams

James Malloy,[1] Erin Marlowe,[1] Christopher J. Jensen,[1] Isaac S. Liu,[1,2] Thomas Hulse,[1,3] Anne F. Murray,[4] Daniel Bryan,[4] Thomas G. Denes,[4] Dustin A. Gilbert,[5] Gen Yin,[1] and Kai Liu[1,*]

[1]*Department of Physics, Georgetown University, Washington, DC 20057*

[2] *Vanderbilt University, Nashville, TN 37235*

[3]*Department of Physics, University of Louisville, Louisville, KY 40292*

[4] *Department of Food Science, University of Tennessee, Knoxville, TN, 37996, USA*

[5]*Materials Science Department, University of Tennessee, Knoxville, TN 37996*

1. Methods

1.1 Isotherm Measurements

Foam surface areas were determined using BET krypton adsorption isotherm measurements with error below 0.5%, carried out by the Particle Testing Authority of Micromeritics Instrument Corp. All samples were placed under vacuum at 200°C for 16 hours to properly degas before measurement.

1.2 Foam Feature Size Analysis

Size analysis of the foam surface features resulted from the 2ED process was performed for a variety of samples by first taking scanning electron microscopy (SEM) images of the foams, and then image-conditioning them using ImageJ to quantify the microstructures using developed algorithms in Python scripts. A flowchart of the full process is shown in Figure S1.

Supplementary Information

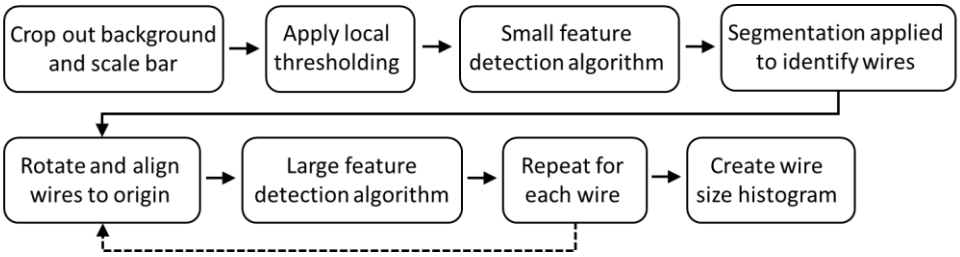

Figure S1: Image analysis flowchart.

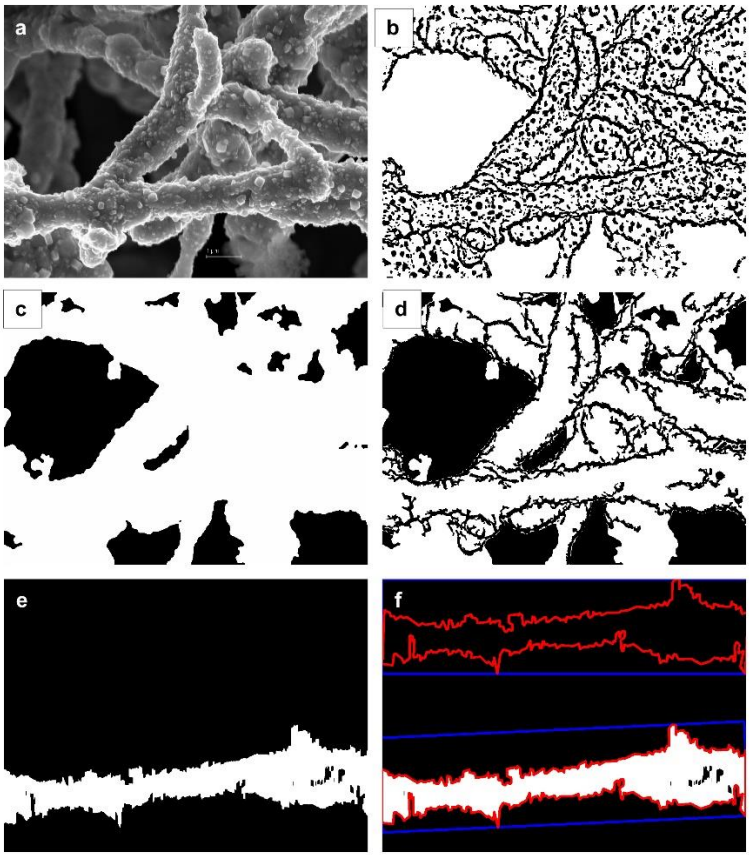

Figure S2: a) Initial image from SEM. b) Image after median auto-local-thresholding. c) Result of image segmentation. d) Large feature boundaries superimposed on segmented image. e) Single wire area extracted by large feature detection algorithm. f) Bounding box and axis-aligned wire outline used to calculate diameter.

Supplementary Information

The SEM images were prepared for analysis by removing the background or any unfocused areas and then removing scale legends and other irrelevant objects so that only features of interest remained. The analysis process began with small-scale feature detection. Separating small features such as nanogranules from 2ED from larger ones such as the nanowires was necessary because the two kinds appeared distinct. Small features appeared in the thresholded image as filled ellipses, whereas large ones would only have their outlines visible and appeared as long trunk-like features.

An *ImageJ* Auto Local Threshold filter using the median method was applied to the image to binarize the image and reveal all features (Fig. S2b). Next, the small feature detection algorithm was run on the binary image. This algorithm found small ellipse features with an area smaller than a threshold amount (such as 1000 pixels) and measured their approximate diameter. Subsequently, the identified small features were removed from the binary image so that only large features remained. The original image was then run through a segmentation filter in *ImageJ* using the *DiameterJ* plugin (Fig. S2c). The outlines of the large features were superimposed to divide the area into individual wires (Fig. S2d). Each wire was then analyzed individually (Fig. S2e). The wire was rotated so that its bounding box is horizontal and the diameter was measured at each pixel along the wire (Fig. S2f). The measured diameters were then averaged for the entire nanowire. This diameter quantification process was repeatedly applied to each nanowire in the input image.

Finally, a feature size distribution histogram was calculated. For every pixel in a feature, the feature diameter was added to the histogram, yielding a correlation between feature diameter and the number of pixels in the image representing features of the corresponding size. The size distribution histograms (Fig. S3), with features between 200-400 nm highlighted in red, can then

be used to determine the feature size evolution of the foams as a function of the 2ED process, which is included in Fig. 4 of the main text.

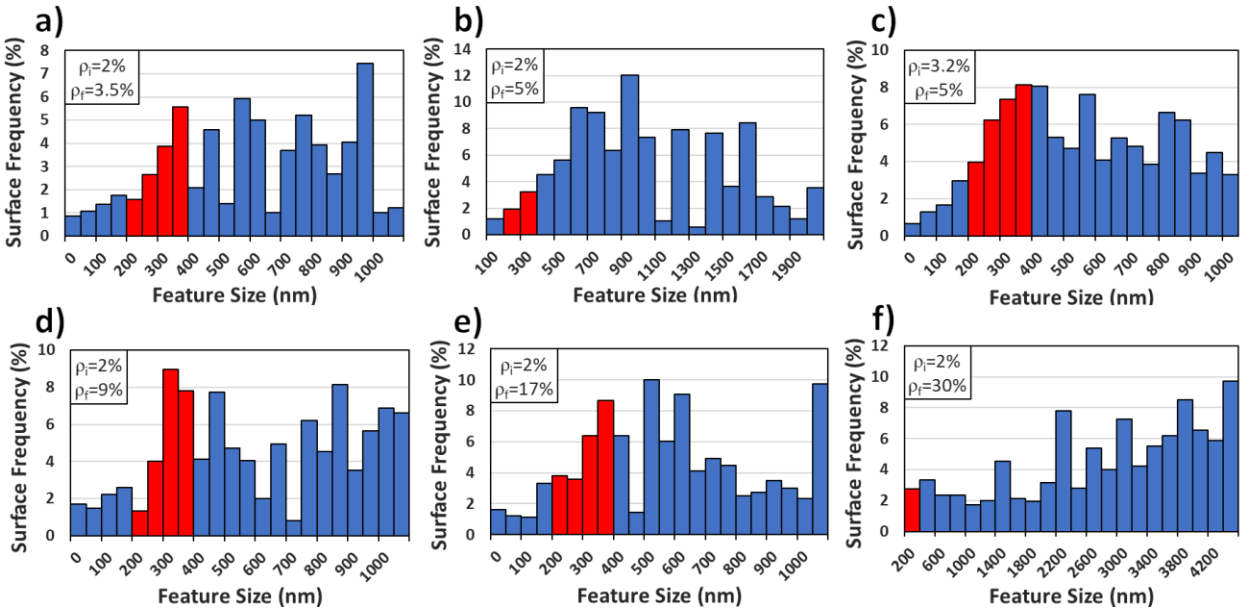

Figure S3: Feature size distribution of foam samples with (a) ρ_i=2%, ρ_f= 3.5%, (b) ρ_i=2%, ρ_f= 5%, (c) ρ_i=3.2%, ρ_f= 5%, (d) ρ_i=2%, ρ_f= 9%, (e) ρ_i=2%, ρ_f=17%, and (f) ρ_i=2%, ρ_f= 30%.

1.3 Pressure Drop Measurement

Pressure differentials between the up-stream/down-stream of the foams were measured while the air flow rate was monitored with a Kelly Pneumatics Air & Oxygen Mass Flow Meter. The face velocity, or the speed at which air flows through the filter (air speeds are between 0 to 1 m/s), was determined by dividing the flow rate by the surface area of the foam. The pressure drop was then measured as a function of face velocities.

Supplementary Information

To determine how key characteristics of the foam influence the breathability, we first model the foam using the single fiber model for the pressure drop.[1] Air filtration theory allows expression of the linear pressure drop coefficient ($\frac{\Delta P}{v}$) as:

$$\frac{\Delta P}{v} = C_{\Delta P} \frac{4\eta t n \cdot f(\rho_f) \cdot f(K_n)}{{d_f}^2} \tag{S1}$$

where η is the coefficient of viscosity, t is the filter thickness, $f(\rho_f)$ is a function dependent on the packing density of the material, n is the nanowire length density, d_f is the nanowire diameter after plating,[1] and $C_{\Delta P}$ is a constant dependent on nanowire spacing geometry and various other factors. The mean free path of the gas molecules (λ) is around 67 nm at standard pressure and temperature. As λ is comparable to the many nanogranular growths along the nanowires as well as the diameter of the nanowires themselves, a significant amount of slip occurs which increases the drag force and is represented by a function of the Knudsen number ($K_n = \frac{2\lambda}{d_f}$).[2] The resulting pressure drop of the foams is found to scale as

$$\frac{\Delta P}{v} \propto \frac{nt \cdot f(\rho_f)}{{d_f}^3} \tag{S2}$$

The $f(\rho_f)$ function used is dependent on the geometry of the nanowires, which for the foams we can use the Miyagi cell model[3] written to a close approximation as:

$$f(\rho_f) \approx \frac{-8 \cdot \rho_f \cdot e^{4.75\rho_f}}{\ln(\rho_f) + \frac{1-{\rho_f}^2}{1+{\rho_f}^2}} \tag{S3}$$

The average diameter of the nanowire before and after the 2ED process increases approximately as $d_f = d_i\sqrt{\frac{\rho_f}{\rho_i}}$, where d_i is nanowire diameter before plating, ρ_i and ρ_f are the initial and final

foam density before and after 2ED, respectively. This can be derived from the volume of a cylinder equation, where $\rho_f \propto \frac{\pi}{4} n {d_f}^2$ and $\rho_i \propto \frac{\pi}{4} n {d_i}^2$. However, as all the nanowires in this study have the same initial diameter prior to plating, this can be simplified to $d_f \propto \sqrt{\frac{\rho_f}{\rho_i}}$. Additionally, the nanowire length density of the foam, which is the sum of the lengths of all the nanowires per given volume, scales as $n \propto \rho_i$, as it is proportional to the number density of nanowires. Combining those into Equations S2 and S3, we find:

$$\frac{\Delta P}{v} \propto -\frac{{\rho_i}^{\frac{5}{2}} \cdot e^{4.75\rho_f} \cdot t}{{\rho_f}^{\frac{1}{2}} \cdot \left[\ln(\rho_f) + \frac{1-{\rho_f}^2}{1+{\rho_f}^2}\right]} \tag{S4}$$

1.4 Foam Efficiency Measurement

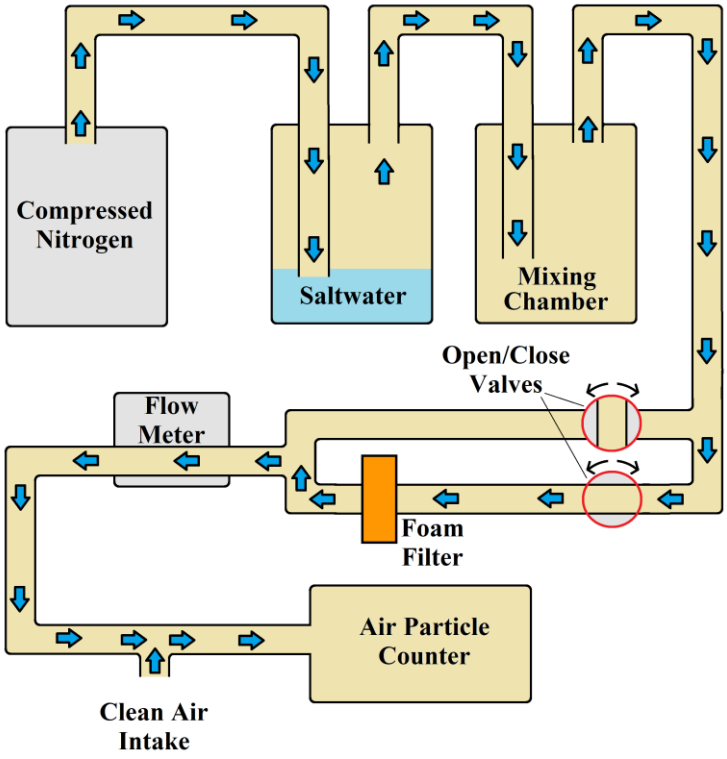

Figure S4: Foam efficiency measurement schematic.

Supplementary Information

Filtration efficiency was measured using a TSI 9110 portable particle counter with the setup depicted below (**Figure S4**). Compressed nitrogen was first flown through a container of stirred saltwater to generate NaCl particles. The NaCl particles were then flown into a large mixing chamber reservoir to keep the particle concentration stable, after which the particles entered into a junction where the open/close valves were positioned to either flow the air through the foam filter, or through an unobstructed path. The flow meter was used to measure the volume of the particle-filled air passing through, and an injection of clean air at atmospheric pressure through the clean air intake was used to bring the air pressure back up to atmospheric pressure and raise the total flow rate passing through the particle counter to 28.3L/min, both of which were required for the particle counter to function properly. As the particle counter was measuring the concentration of particles only after being mixed with clean air, the particle concentration before being mixed was calculated using

$$Q_m \cdot n_f + (Q_T - Q_m) \cdot n_c = Q_T \cdot n_m, \tag{S5}$$

where Q_m was the air flow rate as measured by the flow meter, n_f was the particle concentration flowing past the filter, Q_T was the total air flow passing through the particle detector (28.3L/min), n_c was the particle concentration of the clean air, and n_m was the particle concentration as measured by the particle counter. Solving for n_f, we got:

$$n_f = \frac{Q_T}{Q_m} \cdot (n_m - n_c) + n_c \tag{S6}$$

The efficiency of the filter (E) could then be found by comparing the particle concentration when flowing NaCl particles past the filter, to the particle concentration when unfiltered:

$$E = 1 - [\frac{n_{f(filter)}}{n_{f(no\ filter)}}] \tag{S7}$$

This measurement was repeated several times for each sample to ensure concentration of generated NaCl particles remained stable. The pressure from the compressed nitrogen was used to adjust the air flow through the filter, with measurements typically performed at a flow rate of 0.5-1L/min.

2. Characterizations

2.1 Dependence of foam morphology on electrolyte pH

The pH value of the electroplating solution is important as more acidic solutions will start to etch away the foam during the plating process. This can be used to control the morphology of the foam as the etching is non-uniform. One notable difference is that the amount of copper dissolved in a specific area is correlated with high surface area, which results in acidic plating solutions preferentially targeting the deposited nanogranules and creating foams with smoother nanowires and less overall surface area.

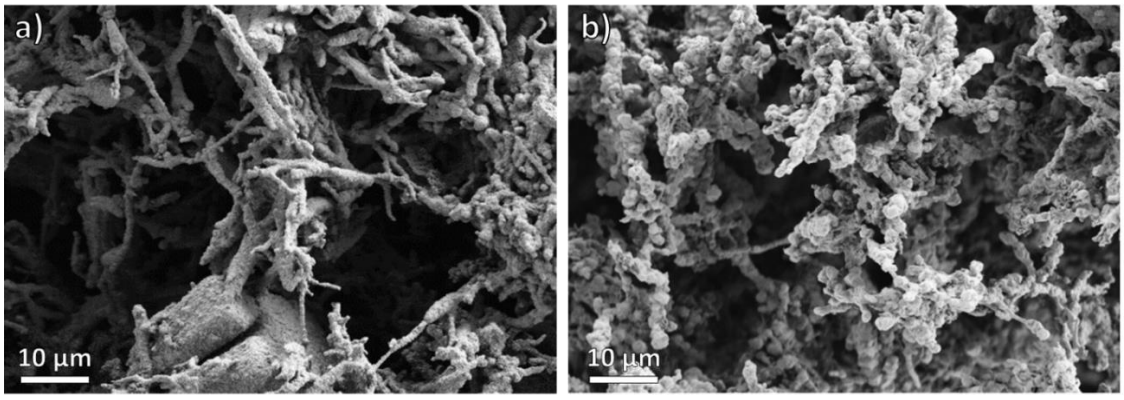

Figure S5. SEM image of (a) exterior surface and (b) interior region of a ρ_f = 9% foam plated at pH of 1-3.

The benefit of this is that the pH can be tuned to maximize the percentage of nanogranules in the 0.3 µm size range. Various foam samples were plated with an electrolyte pH ranging between

1 to 4. The electrolyte becomes more acidic as it is used in multiple depositions. Foam plated with lower pH (≤ 3) electrolyte solutions were found to have smaller diameter nanowires along the exterior and larger diameter nanowires along the interior. The reason for this is that as the electrolyte solution diffuses towards the interior of the foam, it will etch away copper along the way and raise the pH locally as the solution becomes saturated with copper ions. This causes the plating solution in the interior of the foam to become locally less acidic than the solution in the exterior which results in the exterior nanowires being etched at a higher rate and having a disproportionately smaller diameter, as shown in Figure S5.

In cases where the foams were plated with an electrolyte on the higher end of the tested pH range (>3), the reverse trend was observed. Large nanogranules and large diameter nanowires are observed on the exterior of the foam while smooth, narrow nanowires are found in the interior. This is due to the 2ED process preferentially plating the exterior of the foam as result of a larger accumulation of charges. In lower pH solutions this 2ED growth was offset by the acidity of the electrolyte preferentially etching away at the exterior, while in higher pH solutions the 2ED growth prevails. Figure S6 shows a foam electrodeposited at a pH of 3.42, which has large nanogranules on the exterior surface. As the exterior is not being rapidly etched by the electrolyte, copper is able to nucleate on the nanowires. As the granules on the exterior of the foam grow, the electrolyte becomes less saturated with Cu^{2+}, lowering the pH inside the foam. This causes a similar effect to etching of the exterior of the foams plated at lower pH, resulting in narrower, smoother nanowires.

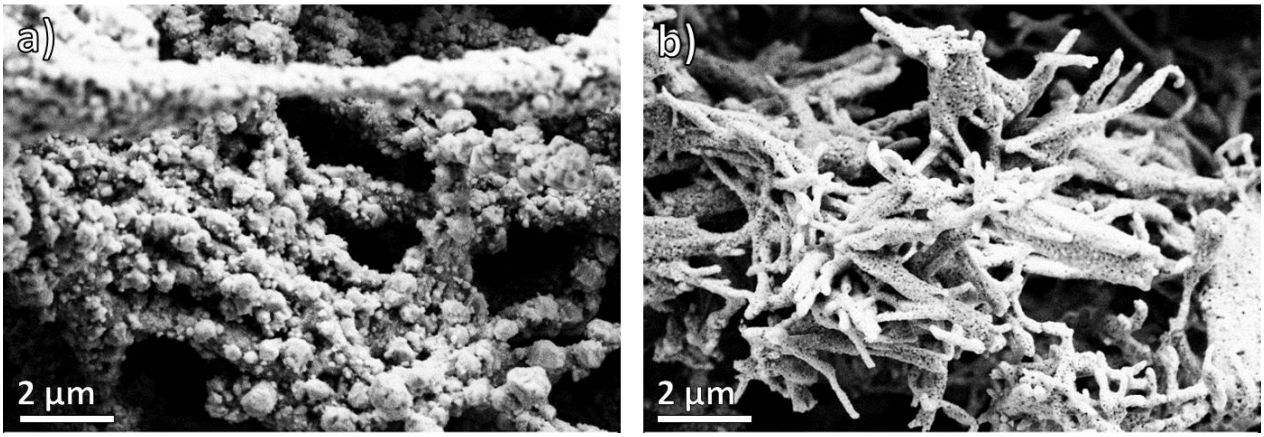

Figure S6. SEM image of (a) exterior surface and (b) interior region of a ρ_f = 9% foam plated at pH of 3.42.

2.2 Quantitative Foam Filtration Characteristics

The calculated surface feature adjusted Filtration Quality (F_{QSF}) was found to be in very close agreement with the measured results, with F_{QSF} generally being within the measurement error range of F_{QE}, as seen in **Table** 1 of the main text. The calculated Quality Factor $Q_{Calculated}$ was also found to be in close agreement with the measured results as well, and this remained true across a wide range of samples. The only sample where the calculated Quality factor is 2 sigma outside the error range of the measured quality factor is in Sample 7, where the likely cause is due to the heavily enhanced surface area as well as altered surface microstructure having a significant effect on the breathability. Any breathability dependence on surface feature microstructure results in the calculated Quality Factor not having as close of a match to the measured results as F_{QSF} does, as the effects of the surface area and surface features on breathability were not examined in this study.

Supplementary Information

2.3 Size Tunability and prototyping

While the foams presented in this study are typically between 5-10 mm in diameter, we have demonstrated that there is no significant limitation on the size that can be manufactured. Pictured below in **Figure S7** is a 1 mm thick foam that is 4 cm in diameter.

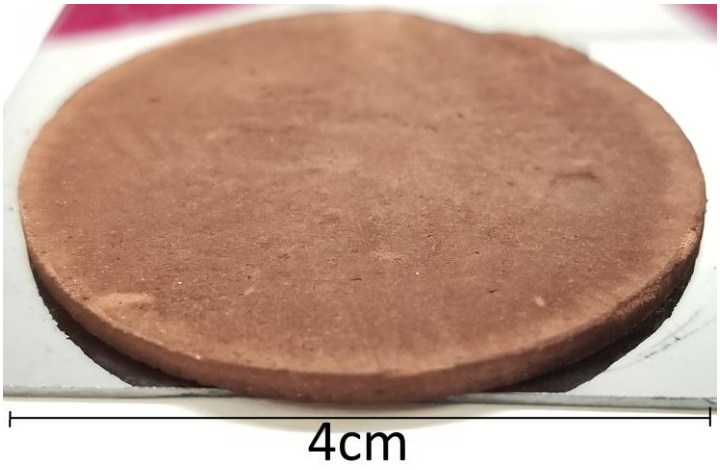

Figure S7. Photo of a 1 mm thick, 4 cm diameter copper foam that was incorporated into a respirator cartridge.

References

(1) Brown, R. *Air Filtration: An Integrated Approach to the Theory and Applications of Fibrous Filters.* 1st ed.; Pergamon Press: 1993.

(2) Lee, S.; Bui-Vinh, D.; Baek, M.; Kwak, D.-B.; Lee, H. *Sci. Rep.* **2023**, *13* (1), 5449.

(3) Miyagi, T. *J. Phys. Soc. Jap.* **1958**, *13* (5), 493-496.